Alteration of Water Structure by Peptide Clusters Revealed by Neutron Scattering in the Small-Angle Region (below 1 $Å^{-1}$)

Isabella Daidone,[†*] Claudio Iacobucci,[†] Sylvia E. McLain,[‡] and Jeremy C. Smith[§¶*]
[†]Department of Physical and Chemical Sciences, University of L'Aquila, L'Aquila, Italy; [‡]Department of Biochemistry, University of Oxford, Oxford, United Kingdom; [§]Oak Ridge National Laboratory, Oak Ridge, Tennessee; and [¶]Department of Biochemistry and Cellular and Molecular Biophysics, University of Tennessee, Knoxville, Tennessee

ABSTRACT Solution scattering of neutrons and x-rays can provide direct information on local interactions of importance for biomolecular folding and structure. Here, neutron scattering experiments are combined with molecular-dynamics simulation to interpret the scattering signal of a series of dipeptides with varying degrees of hydrophobicity (GlyAla, GlyPro, and AlaPro) in concentrated aqueous solution (1:20 solute/water ratio) in which the peptides form large segregates (up to 50–60 amino acids). Two main results are found: 1), the shift to lower Q of the so-called water-ring peak ($Q \approx 2$ $Å^{-1}$) arises mainly from an overlap of water-peptide and peptide-peptide correlations in the region of $1.3 < Q < 2$ $Å^{-1}$, rather than from a shift of the water signal induced by the presence of the clusters; and 2), in the low-Q region ($Q \approx 0.6$ $Å^{-1}$) a positive peak is observed originating from both the solute-solute correlations and changes in the water structure induced by the formation of the clusters. In particular, the water molecules are found to be more connected than in the bulk with hydrogen-bonding directions tangential to the exposed hydrophobic surfaces, and this effect increases with increasing peptide hydrophobicity. This work demonstrates that important information on the (hydrophobic) hydration of biomolecules can be obtained in the very-small-angle region.

INTRODUCTION

The perturbation of water structure by the side chains of amino-acid residues in proteins may play an important role in the thermodynamics of the protein folding process and the determination of protein structure (1–3). Direct protein-water interactions and the perturbation of bulk water by the presence of protein groups are expected to influence folding landscape thermodynamics at different stages of the folding process. In particular, the hydrophobic effect, one of the driving forces in protein folding, is dominated by an entropic component that arises from changes in the structure of the surrounding aqueous environment. Hence, structural and dynamical investigations focused on atomic-level interactions between water and hydrophobic or hydrophilic side chains present in proteins can yield a greater understanding of the mechanism by which proteins fold. In this regard, experiments on solutions of amino acids and small peptides at high concentration (i.e., concentrations at which the solute molecules form clusters) are of special interest because these clusters mimic the conditions expected to be found in the early stages of protein folding.

Information about the hydration structure on the molecular level can be obtained from a wide range of both neutron and x-ray scattering experiments in which local atomic coordination on the Ångström length scale (e.g., neutron and x-ray diffraction) (4–8), or larger-scale macroscopic structures on the nano- to micrometer scale (e.g., small-angle x-ray scattering (SAXS) and small-angle neutron scattering (SANS), respectively) (9–13) can be measured. These measurements can be interpreted with the aid of computer simulation (14–20), allowing in favorable cases a full assessment of the hydration structure from simulations that are consistent with measured experimental data.

In both SANS and SAXS experiments, in which large-scale aggregation is examined, the scattering signal is measured over very small angles corresponding to Q-values ranging between 0.001 and 0.2 $Å^{-1}$ (where $Q = 4\,\pi\,sin\theta/\lambda$; θ is the scattering angle, and λ is the wavelength of the incident neutron or x-ray probe). Details of hydration at the atomic level require measurement over a much wider angular range corresponding to Q-values of 0.01–50 $Å^{-1}$. Measurement on length scales typical of small aggregates (11,21), such as small clusters of amino acids or peptides, is more difficult because it requires larger Q-values than are typically measured by SANS or SAXS yet smaller Q-values than are typically measured in solution diffraction.

Earlier neutron scattering measurements on the hydrophobic amino acid *N*-acetyl-leucine-amide (NALA) in dilute aqueous solutions ($\approx$1:100 solute/water ratio) revealed a shift in the main diffraction peak, or water-ring peak, to lower scattering angles than observed in pure water (9,15). This shift was reproduced by molecular-dynamics (MD) simulation and was attributed primarily to alterations in water-water correlations, i.e., changes in water structure relative to the bulk (9,15). Moreover, x-ray scattering experiments and MD simulation on a more concentrated NALA solution ($\approx$1:25 NALA/water ratio) revealed a further, lower-Q diffraction peak at $Q \approx$ 0.6–0.8 $Å^{-1}$ that was modeled as arising from the scattering of small aggregates of two to six solute molecules (11).

Submitted April 11, 2012, and accepted for publication August 3, 2012.

*Correspondence: daidone@caspur.it or smithjc@ornl.gov

Editor: Bert de Groot.

0006-3495/12/10/1518/7 $2.00

http://dx.doi.org/10.1016/j.bpj.2012.08.010

Together, the scattering and simulation results summarized above lead to two intriguing questions: Is the shift of the water-ring peak to lower scattering angles a general feature of solutions of hydrophobic amino acids, and, in concentrated aqueous solutions of hydrophobic biomolecules, what is the physical origin of the above-mentioned water-ring shift and the appearance of the peak at even lower scattering angles?

To gain insight into these questions, we performed a joint neutron scattering and computational study of three dipeptides in aqueous solution at higher concentrations ($\approx$1:20 solute/water ratio) than employed in the above-cited measurements on NALA (9–11). The three dipeptides studied, glycyl-L-alanine (GlyAla), glycyl-L-proline (GlyPro), and L-alanyl-L-proline (AlaPro), possess increasing hydrophobic character along the series, with GlyAla being the least hydrophobic. Glycine has the smallest hydrophobic group (-H), alanine has a single methyl group (-CH_3), and proline has the largest hydrophobic group with its pyrrolidine ring (-CH(N)$(CH_2)_3$). Proline was chosen for this investigation because it is both hydrophobic and soluble enough to make the neutron diffraction experiments feasible. Note that the peptide bond in GlyAla is a secondary amide, whereas the other two dipeptides are tertiary amides (Fig. 1).

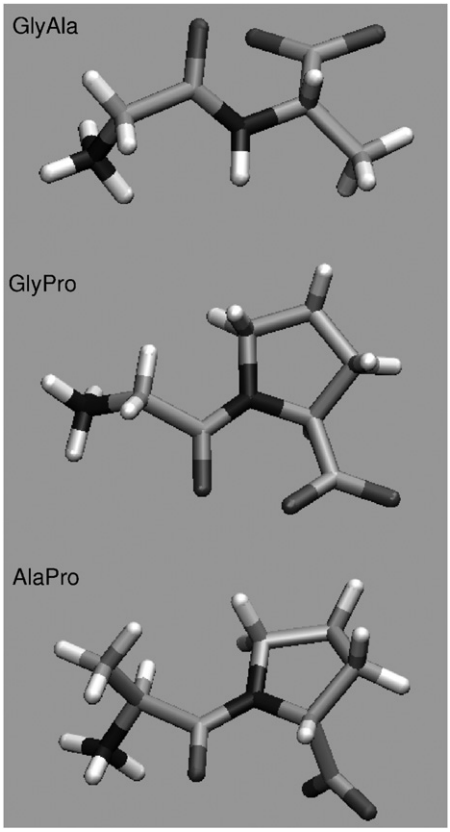

FIGURE 1 Molecular structure of the dipeptides studied.

A previous study (21) showed that these peptides tend to form small aggregates of varying dimensions up to 25–30 dipeptides, and that the driving force for this clustering is hydrophilic in nature (i.e., most of the interpeptide interactions were found to occur between the charged N-terminal and C-terminal ends). Because on average the solvent-exposed surface of the aggregates is 55–60% hydrophobic, these peptide solutions offer good model systems for investigating the hydration of the hydrophobic side chains in a partially aggregated system.

Here, we compute the neutron diffraction profiles of the three dipeptides from long-timescale (microsecond) MD simulations of the corresponding solutions and compare them with the experimental data. The experimental and computed scattering results are found to be in very good agreement, allowing a detailed analysis of the scattering features. Particular attention is given to the presence in all solutions of the clear positive peak in the low-Q region and its relation to the arrangement of the water and peptides, and the evaluation of excluded volume effects (22) on the water signal. The results determine whether or not the solutes modify the solvent structure relative to pure water.

MATERIALS AND METHODS

We performed MD simulations of the three peptides using the GROMACS software package (23) with the AA-OPLS force field (24) for the peptide and the SPC/E model (25) for water in an NVT ensemble at 300 K. The temperature was kept constant with isokinetic temperature coupling (26). The simulation boxes were fixed at the appropriate experimental density at the given temperature and contained 50 peptides and 1000 water molecules in a volume of $\approx$40 nm^3 in each case. We used periodic boundary conditions and treated the electrostatic interactions using the particle mesh Ewald method (real-space cutoff: 0.9 nm) (27). The bond lengths were fixed (28), and a time step of 2 fs was used for numerical integration. Each simulation was performed for 1 μs, with coordinates stored every 1 ps.

We also performed a simulation of pure water (SPC/E) and two simulations of a single GlyPro-shaped molecule with two different sets of partial charges in aqueous solution using the same procedure as described above. A box size similar to that used for the concentrated dipeptide solutions was employed to minimize possible variations in the calculated scattering arising from differences in the box size. The density of the water was set to the density of liquid water at 300 K, and each simulation was 10 ns long.

To generate configurations of pure water in the presence of excluded volume, we adopted the following procedure: First, 100 configurations of the dipeptides generated in the MD simulation (of either the concentrated solution or the infinitely diluted system, depending on the need) were overlaid on 1000 configurations of water molecules extracted from the simulation of pure water (with the box size being the same), and the waters overlapping the excluded volume of the solutes were deleted from the water configurations.

The total static structure factor, F(Q), was computed via Fourier inversion of the total real-space pair correlation function $G(r)$:

$$F(Q) = \frac{4\pi\rho}{Q}\int r(G(r)-1)\sin(Qr)dr \qquad (1)$$

where $G(r)$ is defined as

$$G(r) = \sum c_\alpha c_\beta b_\alpha b_\beta g_{\alpha\beta}(r) \qquad (2)$$

where $c_{\alpha,\beta}$ and $b_{\alpha,\beta}$ are the atomic fraction and scattering length, respectively, of isotope α, β, and $g_{\alpha\beta}(r)$ are the atom-atom pair distribution functions. The scattering length appropriate to deuterium was used to describe heavy water and all exchangeable hydrogens on the solute to match the experimental measurements.

Partial structure factors of a subgroup of atoms (*e.g.*, scattering from the water molecules only) were obtained by Fourier inversion of the weighted sum of the corresponding atom-atom pair distribution functions, $g_{\alpha\beta}(r)$. For example, the water-water partial structure factor $F_{water-water}(Q)$, i.e., the structure factor for all of the water-water interactions, was obtained by Fourier inversion (Eq. 1) of the water-water pair distribution function, $F_{water-water}(Q)$, which is defined as:

$$G_{water-water}(r) = c_{O_w}^2 b_{O_w}^2 g_{O_wO_w}(r) + 2c_{O_w} b_{O_w} c_{H_w} b_{H_w} g_{O_wH_w}(r) + c_{H_w}^2 b_{H_w}^2 g_{H_wH_w}(r) \quad (3)$$

Note that the total static structure factor is the sum of all the partial structure factors present in the system.

It should be pointed out that the large simulation box used (volume $\approx$ 40 nm^3 for each system) and the excellent sampling of the solute configurations in solution achieved (1 μs) allow for an accurate computation of F(Q) in the small-angle region down to $Q = 0.25$ $Å^{-1}$.

Neutron diffraction patterns from GlyAla, GlyPro, and AlaPro in aqueous solutions of D_2O were collected on the SANDALS diffractometer at the Rutherford Appleton Laboratory (ISIS, Chilton, UK). The samples were corrected for multiple scattering, background, and sample container scattering as previously described (21,29).

RESULTS AND DISCUSSION

The solutions of the peptides characterized here are at somewhat higher concentration (one solute to 20 water molecules) than those used in the studies cited in the Introduction, which employed similar but smaller peptides in concentrations ranging from one solute to 25–100 water molecules (9–11). The long MD simulation time (1 μs for each solution) allowed extensive sampling of the systems' configurational space. During the simulations, many possible arrangements of the peptides were observed, ranging from relatively dispersed configurations to aggregated structures, with the cluster size varying from few to 20–30 peptide units (21). Representative structures are shown in Fig. 2 *A*.

The experimental and computed neutron diffraction structure factors, F(Q), for the aqueous solutions of GlyAla, GlyPro, and AlaPro are shown in Fig. 2 *B*. Good agreement is seen between the experimental and computed profiles. In particular, two important features are well reproduced: 1), a slight shift to low Q of the main peak at $Q \approx 2$ $Å^{-1}$ (the so-called water-ring region) on going from the least to the most hydrophobic peptide (with GlyAla and AlaPro being the least and most hydrophobic, respectively); and 2), the presence of a feature at $Q \approx 0.6$ $Å^{-1}$ and its variation along the peptide series, i.e., the intensity was highest for the most hydrophobic (AlaPro) and lowest for the least hydrophobic (GlyAla) species. It should be noted that this low-Q region of measured diffraction data is the most difficult to correct

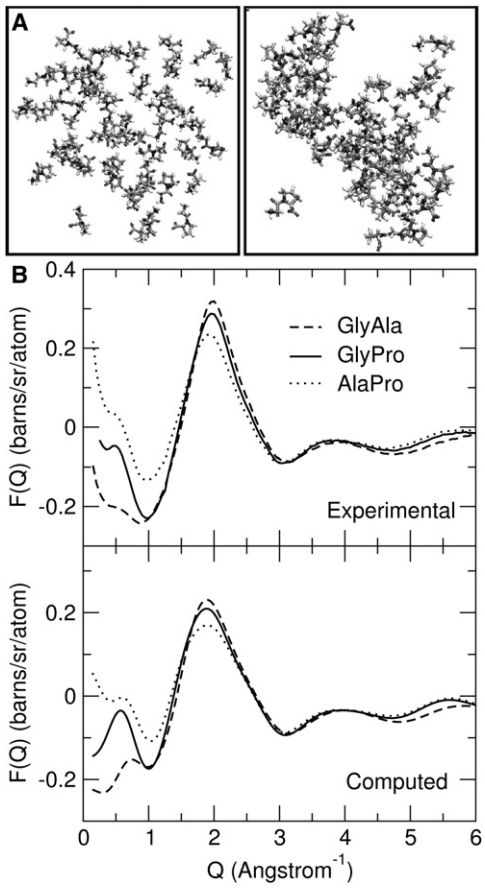

FIGURE 2 (*A*) Representative configurations of the dipeptides in the GlyPro-solution simulation. Examples of rather dispersed (*left*) and more aggregated (*right*) configurations. (*B*) Measured and computed neutron diffraction of the dipeptide systems in aqueous solution. The experimental diffraction patterns were obtained from measurements on these peptides in D_2O as previously reported (21).

for inelastic effects, which therefore may make some contribution to the measured scattering signal shown in Fig. 2 *B*. However, given the similarity in trends between the measured data and the computed F(Q), these effects appear to be small.

We now investigate the relation between the features in the scattering profiles and the arrangement of the water and peptides. First, we present data on the GlyPro solution only (with the results for the other two peptides being consistent with those of the GlyPro system), and subsequently we compare the hydration properties in the three systems. In Fig. 3 *A* the simulation-derived profile of the GlyPro solution is compared with that computed for pure water. As found in previous studies on the amino acid NALA, the water-ring peak is shifted to low Q relative to the corresponding peak in pure water, and also a peak at $Q \approx 0.6$ $Å^{-1}$ is observed (9,11). Fig. 3 *B* shows the decomposition of the computed scattering from the GlyPro solution into its separate components, i.e., arising from water-water, water-solute, and solute-solute correlations

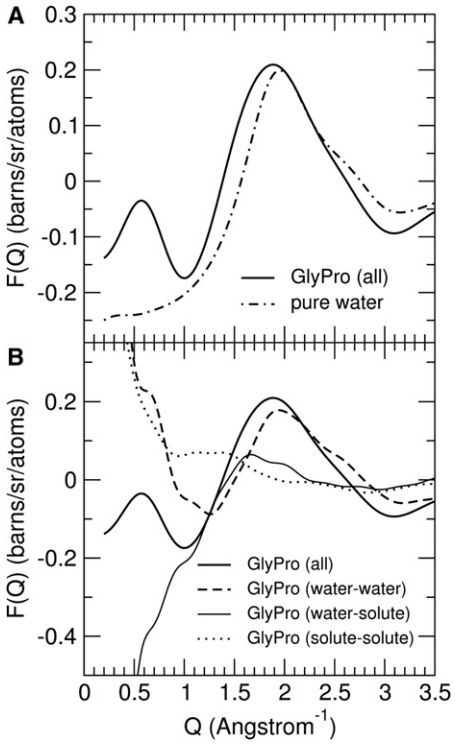

FIGURE 3 (*A*) Computed scattering from the GlyPro solution and pure-water simulations. The pure-water profile was scaled by a factor $k = 0.74$, where k is estimated as the number of water molecules per unit volume of the GlyPro solution divided by the number of water molecules per unit volume of pure water. (*B*) Decomposition of the GlyPro solution scattering into its separate components, i.e., arising from water-water ($F_{water-water}(Q)$), water-solute ($F_{water-solute}(Q)$), and solute-solute ($F_{solute-solute}(Q)$) correlations (see Materials and Methods for the calculation). The thick black curve, which is the same as the thick black curve in panel *A*, is the sum of the other three components. At low Q ($0.25 < Q < 0.50$ Å^{-1}), all three components go off the scale, yet they sum to a finite value. It should be noted that the difference in the scattering pattern of the water molecules in pure water (*A*) and in the GlyPro solution (*B*) arises both from changes in the water structure induced by the presence of the peptides and from the excluded volume of the solutes.

(the latter also includes the intrasolute correlations). Two main aspects emerge: 1), although the water-ring peak does arise mainly from the water-water correlations, clearly also the water-peptide and peptide-peptide correlations contribute to its position and intensity; 2), the peak at $Q \approx 0.6$ Å^{-1} arises from positive contributions of the water-water and peptide-peptide correlations and a negative contribution from the water-peptide correlations.

Changes in the radial distribution functions, and consequently in the scattering pattern, of the solvent molecules can arise from the excluded volume of the solutes, i.e., scattering arising from the water molecules in the presence of peptide-shaped holes. Hence, when the water contribution to the signal from a solution is compared with a pure-water signal with the aim of probing changes in the water structure induced by the presence of the solute, the excluded-volume effect should be taken into account (22). Here, we first analyze the effect of excluded volume on the signal arising from water-water correlations, and then examine in detail the origin of the low-Q peak ($Q \approx 0.6$ Å^{-1}).

To distinguish between the signal arising from the water molecules that were perturbed by the presence of the solutes and pure-water scattering in the presence of excluded volume, we calculated the pure-water scattering including the excluded-volume effect as follows: A series of GlyPro-peptide system configurations sampled in the simulation was overlaid on a series of configurations of pure water, the latter having been simulated in a box of the same size as for the GlyPro solution, and water molecules overlapping the excluded volume of the solutes were deleted from the water configurations (see Materials and Methods for more details). The water configurations thus generated were then used to calculate the radial distribution functions and the corresponding F(Q) signal. In Fig. 4 *A* the scattering from the pure water with the excluded-volume correction is compared with that from the pure water simulation without the correction. The presence of excluded volume is found to affect not only the small-angle region but also partly the water-ring peak in the range $1.3 < Q < 2$ Å^{-1}.

In Fig. 4 *B* the profile of the pure water with excluded volume is compared with the scattering from the water in the GlyPro solution. The position of the water-ring peak in the GlyPro solution almost coincides with that of the pure water with excluded volume, instead of being shifted to lower Q as might be expected from the observation that the total signal arising from all atoms of the solution is indeed shifted toward the left (Fig. 4 *C*). The decomposition of the total scattering into its components shows that the shift in the region $1.3 < Q < 2$ Å^{-1} arises mainly from water-peptide and peptide-peptide correlations (thin-solid and dotted line, respectively, in Fig. 3 *B*), rather than from changes in the water signal itself.

Concerning the lower-Q region, the two profiles (the pure-water-with-excluded-volume profile and the scattering from the water in the GlyPro solution) differ significantly (see Fig. 4 *B*). This indicates that the water signal observed in this region ($Q \approx 0.6$ Å^{-1}) in the GlyPro solution not only arises from the excluded-volume effect, as has been already recognized (10), but also contains a contribution from changes in water structure induced by the presence of the peptide clusters. This finding is mirrored in the corresponding water atom-atom pair distribution functions, $g_{OwOw}(r)$, $g_{OwHw}(r)$, and $g_{HwHw}(r)$ (Fig. 4 *D*), which exhibit small differences in the first hydration shell. In particular, the coordination number is slightly higher (i.e., the peaks are slightly more intense) in the GlyPro solution than in pure water, and around the exposed hydrophobic regions the directions of the hydrogen bonds between the water molecules are tangential to the surface (Fig. 4 *E*). This alteration in the water network leads to the change in the water scattering in the low-Q region.

To analyze the dependence of the water organization on the hydrophobicity of the three dipeptides, the water

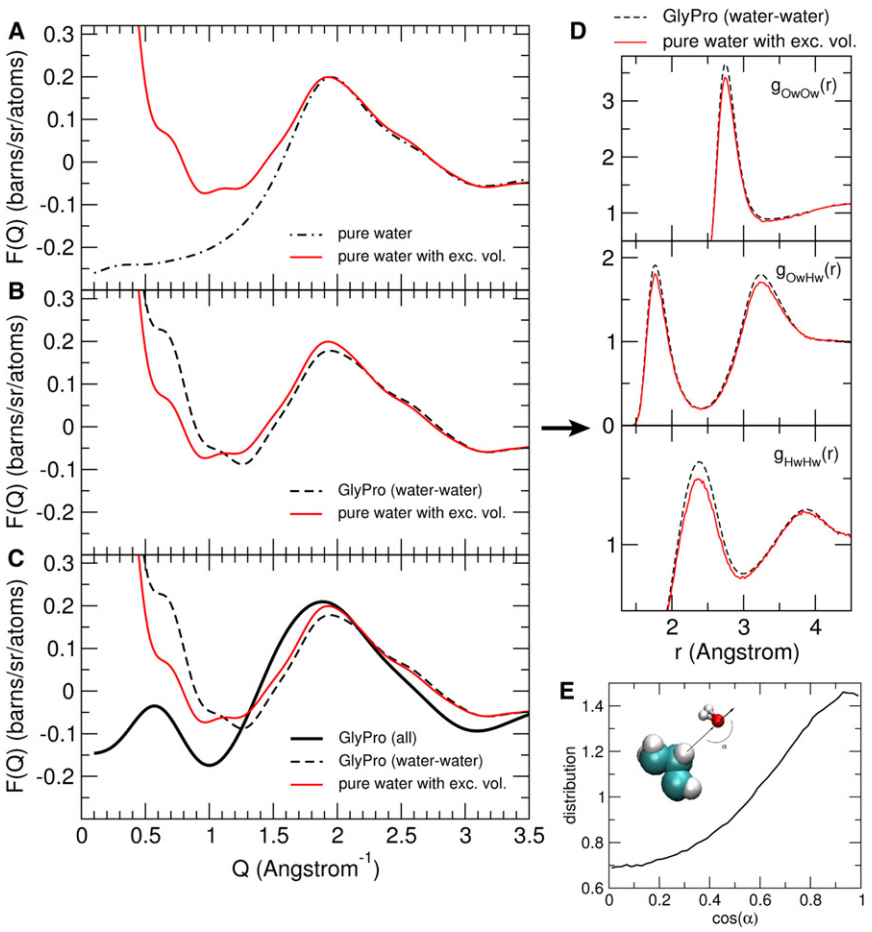

FIGURE 4 Excluded-volume effect on the water signal from the GlyPro dipeptide simulations. (*A*) The pure-water-with-excluded-volume signal (i.e., the scattering of pure water including the excluded-volume correction) is compared with the real pure-water signal (i.e., without the correction). The real pure-water scattering was scaled by a factor $k = 0.74$, where k is estimated as the number of water molecules per unit volume of the GlyPro solution divided by the number of water molecules per unit volume of pure water. (*B*) The pure-water-with-excluded-volume signal is compared with the water signal in the GlyPro solution (GlyPro (water-water)). (*C*) The pure-water-with-excluded-volume signal is compared with the water signal in the GlyPro solution and the total scattering signal of the GlyPro solution (GlyPro (all)). (*D*) Atom-atom pair distribution functions of the water atoms ($g_{OwOw}(r)$, $g_{OwHw}(r)$, $g_{HwHw}(r)$) associated with the water signal in the GlyPro solution (*dashed line*) and with the pure-water-with-excluded-volume signal (*red line*), i.e., the g(*r*) functions associated with the F(*Q*) profiles in panel *B*. (*E*) Structural analysis of the water-molecules arrangement in the GlyPro solution. The distribution of the cosine of the angle, α, between the vector connecting a hydrophobic atom (i.e., belonging to the proline side chains) to the oxygen atom of each water molecule within a distance of 0.5 nm from the considered atom and the normal to the water-molecule plane is shown. A cosine value close to one indicates that the plane of the water molecule is approximately tangential to the surface harboring the considered hydrophobic atom.

atom-atom pair distribution functions, g_{OwOw}(r), g_{OwHw}(r), and g_{HwHw}(r), are computed and compared in the GlyAla, GlyPro, and AlaPro solutions (see Fig. 5). For all three atom-atom pairs, the coordination number increases with increasing hydrophobicity of the peptides, i.e., the peak intensities increase slightly on going from the least to the most hydrophobic peptide (with GlyAla and AlaPro being the least and most hydrophobic, respectively). Hence, the connections between the water molecules are found to increase with increasing hydrophobicity of the peptide.

The above-reported data show that the positive peak at $Q \approx 0.6$ Å^{-1} originates not only from solute-solute correlations but also from changes in the water organization induced by the presence of the clusters. To analyze separately the effect of exposed hydrophilic and hydrophobic patches, and to isolate a pure signature of the hydration of the exposed regions from the more complex signal of a real solution in which the water signal is mixed with the solute-solute correlations, we performed simulations of a single GlyPro molecule in aqueous solution with different charge patterns. Specifically, we chose two different sets of partial charges for the GlyPro molecule: one with all the partial charges set to zero (a hydrophobic analog) and one with enhanced charges (i.e., larger than the standard charges) on the aliphatic carbons and hydrogens (a hydrophilic analog).

The scattering arising from water-water correlations was calculated for the two single-peptide simulations and compared with the corresponding pure-water-with-excluded-volume signal (see Fig. 6). It can be seen that the only difference is in the low-*Q* region, in which the intensity of the signal is highest for the hydrophobic analog and lowest for the hydrophilic analog. These results show that the organization of water molecules around both the hydrophilic and hydrophobic analogs changes relative to that in pure water. However, a signature (i.e., a positive peak) in the low-*Q* region appears only for the hydrophobic species.

The results obtained here raise new possibilities for understanding phenomena that are important in determining biomolecular structure. It is well appreciated that hydration effects are important in this regard (1,10). Hydration contributes to determining the energy landscape for protein folding at all stages in folding, via modification of protein-water and water-water structure. Of particular interest is the modification of water structure, which has been the subject of much debate (3,16,19). Solution scattering is arguably the most direct method for probing structure. However, as this work illustrates, the peaks present in scattering functions

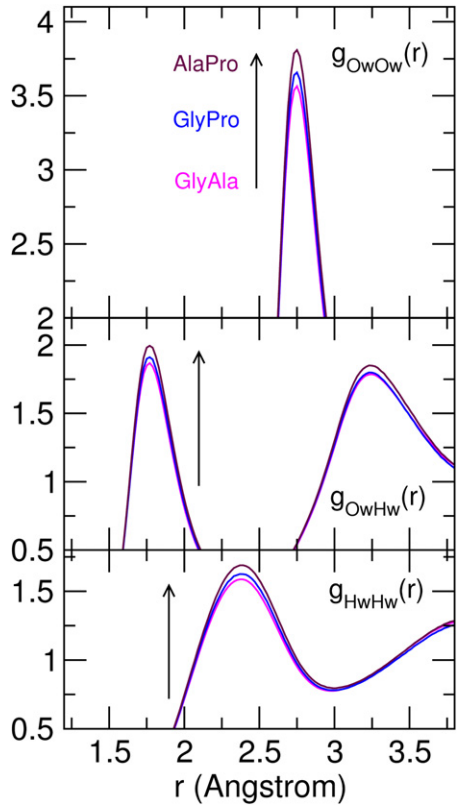

FIGURE 5 Atom-atom pair distribution functions of the water atoms ($g_{OwOw}(r)$, $g_{OwHw}(r)$, and $g_{HwHw}(r)$) in the GlyAla, GlyPro, and AlaPro solutions. The direction of the arrows goes from the least hydrophobic (GlyAla) to the most hydrophobic (AlaPro) peptide.

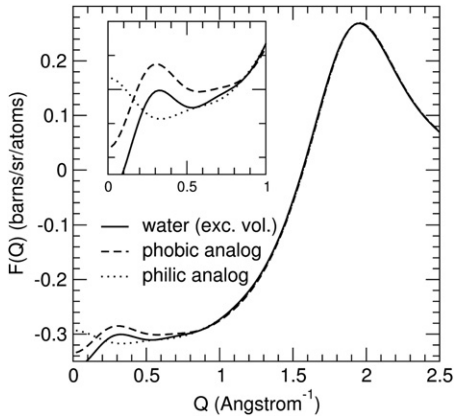

FIGURE 6 Contribution of water to the scattering from a single GlyPro hydrophobic-analog molecule and a single GlyPro hydrophilic-analog molecule in solution. The hydrophobic analog was constructed by taking a GlyPro-shaped molecule with all partial charges set to zero, and the hydrophilic analog was constructed by taking a GlyPro-shaped molecule with enhanced charges (i.e., larger than the standard charges) on the aliphatic carbons and hydrogens. The pure-water-with-excluded-volume signal is also shown for comparison. Here, the excluded volume arises from a single GlyPro-shaped molecule.

can have complex origins, and deciphering these origins requires input from molecular simulation techniques. Here, we have demonstrated that it is possible to decompose peptide solution scattering into contributions from perturbation of water structure and from peptide-water and peptide-peptide interactions.

CONCLUSIONS

In this work, we investigated aqueous solutions of weakly hydrophobic dipeptides (GlyAla, GlyPro, and AlaPro) at a rather high concentration (1:20 solute/water ratio) by means of neutron scattering experiments and MD simulation. Because the peptides reversibly form aggregates of various sizes (from a few to 50–60 amino acids) with, on average, 55–60% of hydrophobic solvent-exposed surface, these solutions offer good model systems with which to investigate the hydrophobic hydration of partially clustered polypeptide chains. Such a system can serve as a mimic of a partially folded protein at the early stages of the folding process, in which the first hydrophobic clusters start to form.

Two important features of the experimental neutron scattering patterns are well reproduced in the computed profiles: 1), the slight shift to low Q of the main water-ring peak at $Q \approx 2$ Å^{-1}; and 2), the increase of intensity of the smaller peak at $Q \approx 0.6$ Å^{-1} on going from the least hydrophobic (GlyAla) to the most hydrophobic (AlaPro) peptide. We drew conclusions about the origin of these features by taking into account the excluded-volume effect (22) when we compared the water scattering signal (and the associated distribution functions) of the peptide solutions with the corresponding signal in pure water. If excluded-volume effects are not considered, conclusions about the effect of a particular solute on the solvent structure may be erroneous.

Concerning the main water-ring peak at $Q \approx 2$ Å^{-1} in the peptide solutions, we found that the shift to lower Q relative to the position in pure water arose mainly from a positive contribution of water-peptide and peptide-peptide correlations in the region of $1.3 < Q < 2$ Å^{-1}, rather than from changes in the water signal itself. In contrast, we found that the peak at $Q \approx 0.6$ Å^{-1} originated not only from solute-solute correlations but also from changes in the water organization induced by the presence of the clusters. In particular, the water network was found to be more connected, i.e., with a slightly higher coordination number between the water molecules, than in bulk water with hydrogen-bonding directions tangential to the exposed hydrophobic surfaces, similarity to solid clathrate hydrates (3,30). Moreover, the degree of connection of the hydrogen-bonding network of the water molecules was found to increase with increasing hydrophobicity of the peptide. These results are relevant for the meaning of hydrophobicity in biomolecular systems.

The data presented here point a way forward for neutron scattering applications in protein folding and beyond. With

regard to folding, clearly the work can be generalized to study polypeptide chains in different stages of folding and indifferent solvents. Effects of temperature and pressure can be probed. Furthermore, the combined MD/diffraction approach demonstrated here can be applied to decipher hydration interactions in many other types of soluble biomolecule. However, we emphasize the need to incorporate simulation and to calculate scattering quantities, rather than derived quantities, directly from the simulation results.

Finally, hydrophobic (rather than hydrophilic) hydration contributes mostly to the increased scattering intensity in the low-Q region. Hence, these data demonstrate that important information about the (hydrophobic) hydration of clusters of peptides can be mined in the small-angle region.

I.D. received financial support from the Consorzio Interuniversitario per le Applicazioni di Supercalcolo Per Universitá e Ricerca through the "Theoretical study of electron transfer reactions in complex atomic-molecular systems" project. J.C.S. received funding from the Molecular and Cellular Biosystems Cluster, National Science Foundation.

REFERENCES

1. Berne, B. J., J. D. Weeks, and R. Zhou. 2009. Dewetting and hydrophobic interaction in physical and biological systems. *Annu. Rev. Phys. Chem.* 60:85–103.
2. Rasaiah, J. C., S. Garde, and G. Hummer. 2008. Water in nonpolar confinement: from nanotubes to proteins and beyond. *Annu. Rev. Phys. Chem.* 59:713–740.
3. Rossky, P. J. 2010. Exploring nanoscale hydrophobic hydration. *Faraday Discuss.* 146:13–18., discussion 79–101., 395–401.
4. Bowron, D. T., J. L. Finney, and A. K. Soper. 1998. Structural investigation of solute-solute interactions in aqueous solutions of tertiary butanol. *J. Phys. Chem. B.* 102:3551–3563.
5. Hulme, E. C., A. K. Soper, …, J. L. Finney. 2006. The hydration of the neurotransmitter acetylcholine in aqueous solution. *Biophys. J.* 91:2371–2380.
6. McLain, S. E., A. K. Soper, …, A. Watts. 2007. Structure and hydration of L-proline in aqueous solutions. *J. Phys. Chem. B.* 111:4568–4580.
7. Mason, P. E., G. W. Neilson, …, J. W. Brady. 2010. Observation of pyridine aggregation in aqueous solution using neutron scattering experiments and MD simulations. *J. Phys. Chem. B.* 114:5412–5419.
8. Pagnotta, S. E., S. E. McLain, …, M. A. Ricci. 2010. Water and trehalose: how much do they interact with each other? *J. Phys. Chem. B.* 114:4904–4908.
9. Pertsemlidis, A., A. M. Saxena, …, R. M. Glaeser. 1996. Direct evidence for modified solvent structure within the hydration shell of a hydrophobic amino acid. *Proc. Natl. Acad. Sci. USA.* 93:10769–10774.
10. Pertsemlidis, A., A. K. Soper, …, T. Head-Gordon. 1999. Evidence for microscopic, long-range hydration forces for a hydrophobic amino acid. *Proc. Natl. Acad. Sci. USA.* 96:481–486.
11. Sorenson, J. M., G. Hura, …, T. Head-Gordon. 1999. Determining the role of hydration forces in protein folding. *J. Phys. Chem. B.* 103:5413–5426.
12. Svergun, D. I., S. Richard, …, G. Zaccai. 1998. Protein hydration in solution: experimental observation by x-ray and neutron scattering. *Proc. Natl. Acad. Sci. USA.* 95:2267–2272.
13. Paciaroni, A., A. Orecchini, …, F. Sacchetti. 2008. Fingerprints of amorphous icelike behavior in the vibrational density of states of protein hydration water. *Phys. Rev. Lett.* 101:148104.
14. Tarek, M., G. J. Martyna, and D. J. Tobias. 2000. Amplitudes and frequencies of protein dynamics: analysis of discrepancies between neutron scattering and molecular dynamics simulations. *J. Am. Chem. Soc.* 122:10450–10451.
15. Head-Gordon, T., J. M. Sorenson, …, R. M. Glaeser. 1997. Differences in hydration structure near hydrophobic and hydrophilic amino acids. *Biophys. J.* 73:2106–2115.
16. Daidone, I., M. B. Ulmschneider, …, J. C. Smith. 2007. Dehydration-driven solvent exposure of hydrophobic surfaces as a driving force in peptide folding. *Proc. Natl. Acad. Sci. USA.* 104:15230–15235.
17. Giovambattista, N., C. F. Lopez, …, P. G. Debenedetti. 2008. Hydrophobicity of protein surfaces: Separating geometry from chemistry. *Proc. Natl. Acad. Sci. USA.* 105:2274–2279.
18. Wood, K., A. Frölich, …, M. Weik. 2008. Coincidence of dynamical transitions in a soluble protein and its hydration water: direct measurements by neutron scattering and MD simulations. *J. Am. Chem. Soc.* 130:4586–4587.
19. Godec, A., J. C. Smith, and F. Merzel. 2011. Increase of both order and disorder in the first hydration shell with increasing solute polarity. *Phys. Rev. Lett.* 107:267801.
20. Chopra, G., and M. Levitt. 2011. Remarkable patterns of surface water ordering around polarized buckminsterfullerene. *Proc. Natl. Acad. Sci. USA.* 108:14455–14460.
21. McLain, S. E., A. K. Soper, …, A. Watts. 2008. Charge-based interactions between peptides observed as the dominant force for association in aqueous solution. *Angew. Chem. Int. Ed. Engl.* 47:9059–9062.
22. Soper, A. K. 1997. The excluded volume effect in confined fluids and liquid mixtures. *J. Phys. Condens. Matter.* 9:2399–2410.
23. van der Spoel, D., R. van Drunen, and H. J. C. Berendsen. 1994. GROningen MAchine for Chemical Simulation. Department of Biophysical Chemistry, BIOSON Research Institute, Nijenborgh 4 NL-9717 AG Groningen. http://www.gromacs.org.
24. Kaminski, G. A., R. A. Friesner, …, W. L. Jorgensen. 2001. Evaluation and reparametrization of the OPLS-AA force field for proteins via comparison with accurate quantum chemical calculations on peptides. *J. Phys. Chem. B.* 105:6474–6487.
25. Berendsen, H. J. C., J. R. Grigera, and T. P. Straatsma. 1987. The missing term in effective pair potentials. *J. Phys. Chem.* 91:6269–6271.
26. Brown, D., and J. H. R. Clarke. 1984. A comparison of constant energy, constant temperature, and constant pressure ensembles in molecular dynamics simulations of atomic liquids. *Mol. Phys.* 51:1243–1252.
27. Darden, T., D. York, and L. Pedersen. 1993. Particle mesh Ewald: an N-log(N) method for Ewald sums in large systems. *J. Chem. Phys.* 98:10089–10092.
28. Hess, B., H. Bekker, …, J. G. E. M. Fraaije. 1997. LINCS: a linear constraint solver for molecular simulations. *J. Comput. Chem.* 18: 1463–1472.
29. McLain, S. E., A. K. Soper, and A. Watts. 2008. Water structure around dipeptides in aqueous solutions. *Eur. Biophys. J.* 37:647–655.
30. Loveday, J. S., and R. J. Nelmes. 2008. High-pressure gas hydrates. *Phys. Chem. Chem. Phys.* 10:937–950.